JOURNAL OF PHYSICAL ORGANIC CHEMISTRY
J. Phys. Org. Chem. 2000; **13:** 313–321

Hammett–Taft cross-interaction correlations for the inhibition mechanism of cholesterol esterase by substituted phenyl *N*-substituted carbamates

Gialih Lin*

Department of Chemistry, National Chung-Hsing University, Taichung 402, Taiwan

Received 25 November 1999; revised 25 January 2000; accepted 13 February 2000

ABSTRACT: With the modified Hammett–Taft cross-interaction variations, multiple linear regressions of the chemical shifts of NH protons, pK_a, log$k_{[OH]}$, $-\log K_i$, logk_c and logk_i values for both substituted phenyl *N*-*n*-butyl carbamates (1) and 4-nitrophenyl-*N*-substituted carbamates 2 give linear correlations, and the cross-interaction constants are -0.5, 0.3, -2.4, 2, 1 and 2, respectively. The cross-interaction constant for the correlation of the chemical shifts of NH protons indicates that the pseudo-*trans* conformers are major conformers of carbamates 1 and 2 in $CDCl_3$. Thus, the distances between the substituents at nitrogen and phenyl of carbamates 1 and 2 are relatively longer. In the transition states of protonations of carbamates 1 and 2 in aqueous solution (pK_a), those distances are also longer. However, those distances of transition states for the *E*1*cB* mechanism of the basic hydrolysis of carbamates 1 and 2 and for the cholesterol esterase inhibition mechanism by carbamates 1 and 2 are relatively shorter based on large absolute values of cross-interaction constants. Moreover, the cholesterol esterase inhibition mechanism by carbamates 1 and 2 is common in the formation of the tetrahedral intermediate and then the carbamyl enzyme. Based on the stereoelectronic effects, the x-ray structures of cholesterol esterase and large values of the corss-interaction constants, the inhibition mechanism of cholesterol esterase by carbamates 1 and 2 is proposed. Copyright © 2000 John Wiley & Sons, Ltd.

KEYWORDS: Hammett–Taft cross-interactions; cholesterol esterase inhibition; carbamate inhibitors

INTRODUCTION

Physiological substrates of cholesterol esterase (CEase) (EC 3.1.1.13), also known as bile salt-activated lipase include cholesteryl esters, retinyl esters, acylglycerols, vitamin esters and phospholipids.[1–4] CEase plays a role in digestive lipid absorption in the upper intestinal tract, although its role in cholesterol absorption in particular is controversial.[5–7] A recent report indicates that CEase is directly involved in lipoprotein metabolism, in that the enzyme catalyzes the conversion of large low-density lipoproteins (LDL) to smaller, denser, more cholesteryl ester-rich lipoproteins, and that the enzyme may regulate serum cholesterol levels.[8] CEase shares the same catalytic machinery as serine proteases[9] in that they have an active site serine residue which, with a histidine and an aspartic or glutamic acid, forms a catalytic triad. The conservation of this catalytic triad suggests that as well as sharing a common mechanism for substrate hydrolysis, that is, formation of a discrete acyl enzyme intermediate via the serine hydroxyl group, serine proteases, CEase and lipases may well be expected to be inhibited by the same classes of mechanism-based inhibitors. Two different x-ray crystal structures of bovine pancreatic CEase have been reported recently.[10,11] Although different bile salt-activation mechanisms for CEase are proposed, the shape of the active site is similar to that of lipases.

In the presence of substrate, the mechanism of pseudo-substrate inhibitions of CEase has been proposed (Scheme 1 and Fig. 1).[12–19] Because the inhibition of CEase follows first-order kinetics over the observed time period for the steady-state kinetics, the rate of hydrolysis of EI′ must be significantly slower than the rate of formation of EI′ (k_c k_3).[20]

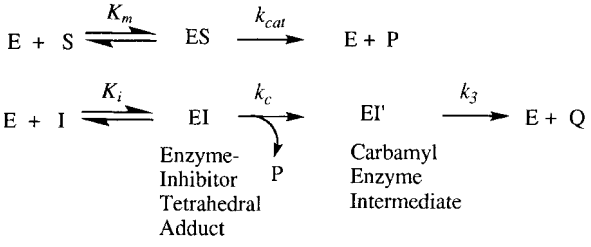

Scheme 1. Kinetic scheme for pseudo-substrate inhibition of CEase in the presence of substrate and inhibitor

**Correspondence to:* G. Lin, Department of Chemistry, National Chung-Hsing University, Taichung 402, Taiwan.
Contract/grant sponsor: National Science Council of Taiwan.

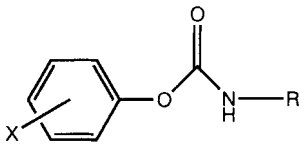

1 : R = *n*-C_4H_9; varied X
2 : X = *p*-NO_2; varied R

Figure 1. Structures of carbamates **1** and **2**

The active site of CEase contains at least four major sub-domains (Fig. 1):[11,12,17–19] (a) the first acyl chain binding site (ACS) that binds to the acyl chain of cholesteryl ester or the first acyl chain of triacylglycerol, (b) the oxyanion hole (OH) A195, G107 and A108 that stabilizes the carbonyl group of the substrate or inhibitor, (c) the esteric site (ES), comprising the catalytic triad S194, H435 and D320, that catalyzes the reaction, and (d) the second acyl chain binding site (SACS) that binds to the cholesteryl part of the cholesteryl ester or the second acyl chain of triacylglycerol.[19] Therefore, the pseudo-substrate inhibition of CEase by carbamates **1** and **2** has been proposed (Fig. 1 and Scheme 1)[12–19]

Structure–reactivity relationships for the inhibition of CEase by aryl carbamates have been demonstrated as important probes to understand the inhibition mechanism.[12–19] The Hammett, Taft–Ingold and Järv–Hansch correlations have been extensively used to study the inhibition mechanism of CEase. However, no cross-interaction effect between two substituents in aryl carbamates has been taken into account. Therefore, we first apply the cross-interaction effect to the structure–reactivity relationships for the inhibition of CEase by carbamates **1** and **2**.

Interactions between substituents (cross-interaction) have been derived from a multiple Hammett correlation:

$$\log(k_{XY}/k_{HH}) = \rho_X\sigma_X + \rho_Y\sigma_Y + \rho_{XY}\sigma_X\sigma_Y \quad (1)$$

where ρ_{XY} is the cross-interaction constant.[21–27] Lee and co-workers[21–23] consider ρ_{XY} to be a measure of the distance between groups X and Y in the transition state and have developed empirical relationships between the cross-interaction constant and intramolecular distance ($|\rho_{XY}|$ varies inversely with distance between substituents X and Y). However, the cross-interaction phenomenon is limited to systems with two substituted phenyl groups. In other words, Eqn. (1) can only apply the Hammett substituent constants (σ)[24–27] to disubstituted phenyl compounds. In this work, we tried to apply the cross-interaction effect to carbamates **1** and **2** that vary the substituents both at the phenyl group and at nitrogen. In other words, we report the cross-interaction effect between σ and the Taft substituent constants (σ^*)[24–27]

RESULTS

The pK_a, log$k_{[OH]}$ and δ_{NH} values of carbamates **1** and **2** and the $-\log K_i$ and logk_i values for the inhibition of CEase by carbamates **1** and **2** do not correlate with the equation

$$\log(k_{XR}) = \text{constant} + \rho_X\sigma_X + \rho^*\sigma^* + \rho_{XR}\sigma_X\sigma^* \quad (2)$$

where σ_X, σ^* and ρ_{XR} are the Hammett substitutent

Table 1. Substitutent constants and kinetic data for inhibitions of CEase by carbamates **1** and **2**

X[a]	R[a]	σ	σ^*	$\alpha\ \sigma\ \sigma^*$[b]	K_i (μM)[c]	k_c (10^{-3} s^{-1})[c]	k_i (M^{-1} s^{-1})[c]
p-OMe	*n*-Bu	−0.27	−0.13	0.035	$(7 \pm 1) \times 10^3$	5.4 ± 0.4	0.8 ± 0.1
H	*n*-Bu	0	−0.13	0	740 ± 70	5.0 ± 0.3	6.7 ± 0.8
m-OMe	*n*-Bu	0.12	−0.13	−0.016	390 ± 30	4.5 ± 0.3	12 ± 1
p-Cl	*n*-Bu	0.23	−0.13	−0.030	82 ± 8	4.4 ± 0.2	54 ± 6
m-Cl	*n*-Bu	0.37	−0.13	−0.048	120 ± 10	4.3 ± 0.2	36 ± 3
m-CF_3	*n*-Bu	0.43	−0.13	−0.056	35 ± 5	4.4 ± 0.2	120 ± 20
p-CF_3	*n*-Bu	0.54	−0.13	−0.070	4.4 ± 0.3	4.2 ± 0.2	960 ± 80
m-NO_2	*n*-Bu	0.71	−0.13	−0.092	3.6 ± 0.3	4.0 ± 0.2	1,100 ± 100
p-NO_2	*n*-Bu	0.78	−0.13	−0.10	2.6 ± 0.3	3.8 ± 0.2	1,500 ± 100
p-NO_2	*n*-Bu	0.78	−0.13	−0.26	2.6 ± 0.3	3.8 ± 0.2	1,500 ± 100
p-NO_2	*n*-Pr	0.78	−0.12	−0.24	2.9 ± 0.3	3.74 ± 0.04	1,300 ± 100
p-NO_2	Et	0.78	−0.10	−0.20	3.1 ± 0.3	3.85 ± 0.03	1,200 ± 100
p-NO_2	*n*-Hex	0.78	−0.15	−0.30	3.2 ± 0.4	3.00 ± 0.03	900 ± 100
p-NO_2	*n*-Oct	0.78	−0.13	−0.26	3.6 ± 0.4	3.75 ± 0.04	1,000 ± 100
p-NO_2	C_2H_4Cl	0.78	0.39	0.77	5.8 ± 0.7	1.21 ± 0.04	210 ± 30
p-NO_2	CH_2Ph	0.78	0.22	0.44	4.4 ± 0.5	8.81 ± 0.09	2,000 ± 200
p-NO_2	Allyl	0.78	0.1	0.20	3.8 ± 0.5	6.00 ± 0.05	1,600 ± 200

[a] The substituents R and X of carbamates **1** and **2** (Fig. 1).[34]
[b] For carbamates **1**, $\alpha = 1$; for carbamates **2**, $\alpha = 2.54$.[25]
[c] Obtained from fitting the k_{app} values of Eqn. (4) (see Experimental).[12]

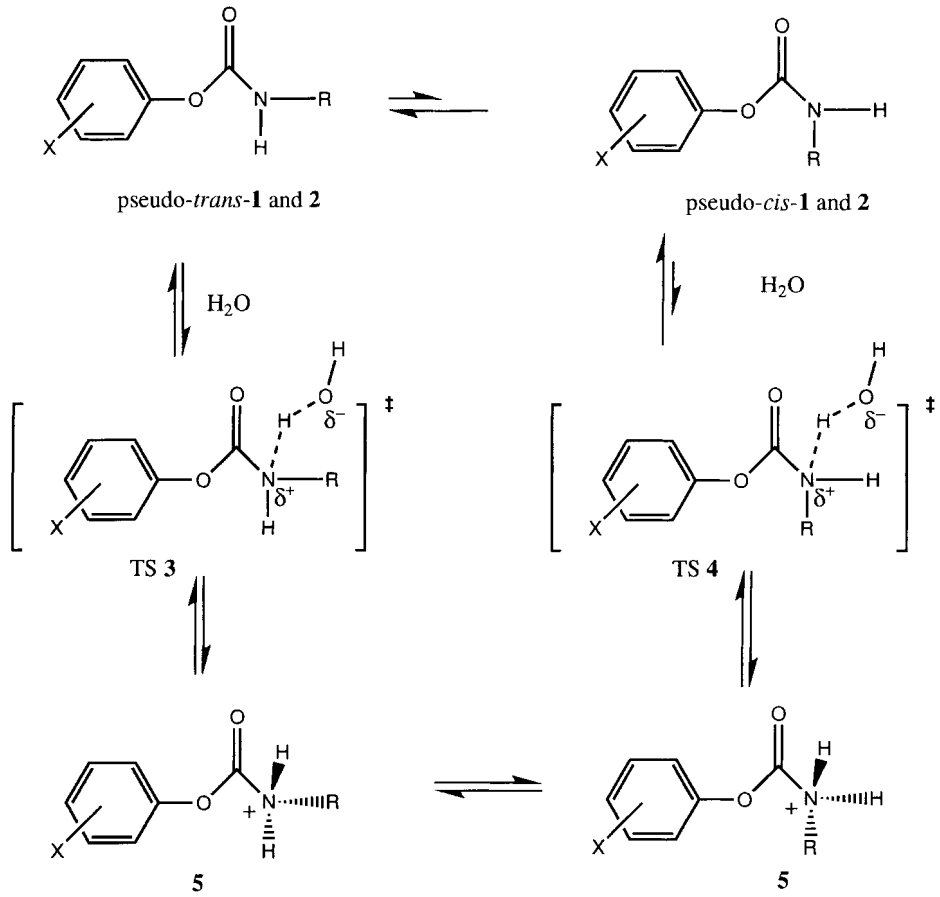

Figure 2. Mechanism for the protonation of carbamates **1** and **2** in aqueous solution

constant, the Taft substitutent constant and the Hammett–Taft cross-interaction constant, respectively.

However, values of pK_a, log$k_{[OH]}$, δ_{NH}, $-\log K_i$, logk_c and logk_i correlate with the equation

$$\log(k_{XR}) = \text{constant} + \rho_X\sigma_X + \rho^*\sigma^* + \rho_{XR}\alpha\sigma_X\sigma^* \quad (3)$$

where α is the weighing factor of the cross-interaction term. The α value is defined to be 1 when R is *n*-C_4H_9 and X is varied (carbamates **1**) and 2.54 when X is *p*-NO_2 and R is varied (carbamates **2**) (Table 1).

The results of these multiple linear correlations are summarized in Table 2. Therefore, the mechanisms for carbamates **1** and **2** with respect to the pK_a, log$k_{[OH]}$, δ_{NH}, $-\log K_i$, logk_c and logk_i systems are common. Moreover, the ρ_{XR} values of pK_a, log$k_{[OH]}$, δ_{NH}, $-\log K_i$, logk_c and logk_i correlations are 0.3, −2.54, −0.5, 2, 1 and 2, respectively. The $|\rho_{XR}|$ values for pK_a and δ_{NH} are <1 but those for log$k_{[OH]}$, $-\log K_i$, logk_c and logk_i are >1.

Table 2. Cross-interaction analyses of structure–reactivity relationships for δ_{NH}, pK_a and log$k_{[OH]}$ of carbamates **1** and **2** and the inhibition of CEase by carbamates **1** and **2**[a]

Parameters	δ_{NH}[b]	pK_a	Log$k_{[OH]}$	$-$LogK_i	Logk_c	Logk_i
ρ	0.08 ± 0.08	9.8 ± 0.1	2.3 ± 0.2	3.7 ± 0.4	0.0 ± 0.5	3.6 ± 0.5
ρ^*	1.8 ± 0.5	-1.5 ± 0.7	6 ± 1	-4 ± 2	-0.5 ± 0.2	-4 ± 3
ρ_{XR}[c]	0.5 ± 0.2	0.3 ± 0.3	-2.4 ± 0.5	2 ± 1	1 ± 1	2 ± 1
h	5.21 ± 0.07	9.8 ± 0.1	4.3 ± 0.2	2.5 ± 0.3	-2 ± 1	0.3 ± 0.4
R[d]	0.9759	0.9983	0.9965	0.9838	0.8892	0.9661

[a] For carbamates **1** and **2** the Eqn. (3) ($\log k_{XR} = h + \rho\ \sigma + \rho^*\ \sigma^* + \rho_{XR}\ \alpha\ \sigma^*\sigma$; $\alpha = 1$ for carbamates **1;** $\alpha = 2.54$ for carbamates **2**) is used in correlations.
[b] All ^{1}H chemical shifts (δ, ppm) are referred to internal TMS (300 MHz, $CDCl_3$).
[c] Cross-interaction constant.
[d] Correlation coefficient.

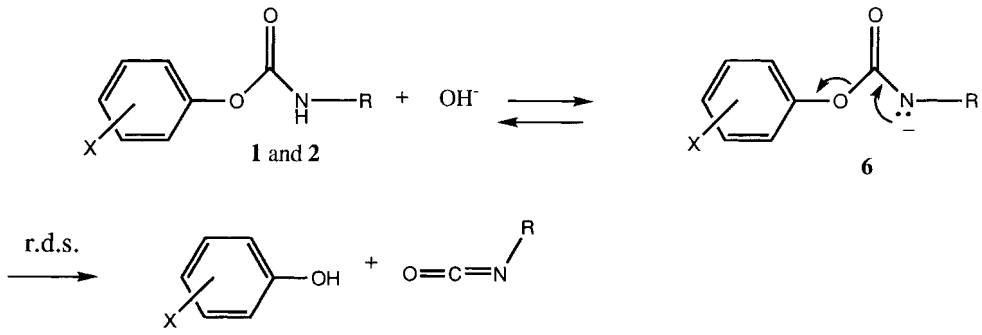

Figure 3. Alkaline-catalyzed hydrolysis of carbamates **1** and **2** via *E*1*cB*[28–30]

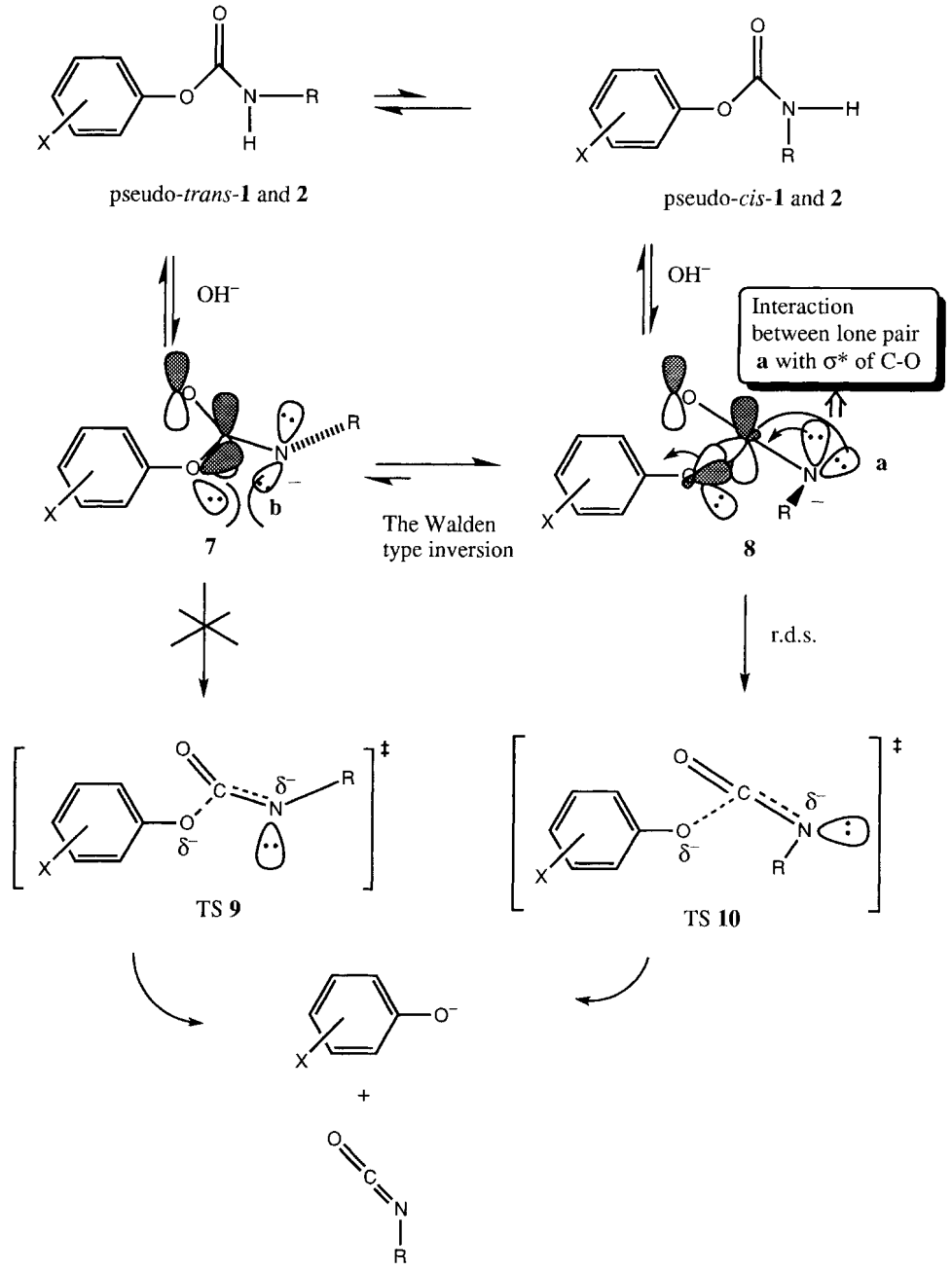

Figure 4. Mechanism for the alkaline-catalyzed hydrolysis of carbamates **1** and **2** via *E*1*cB*

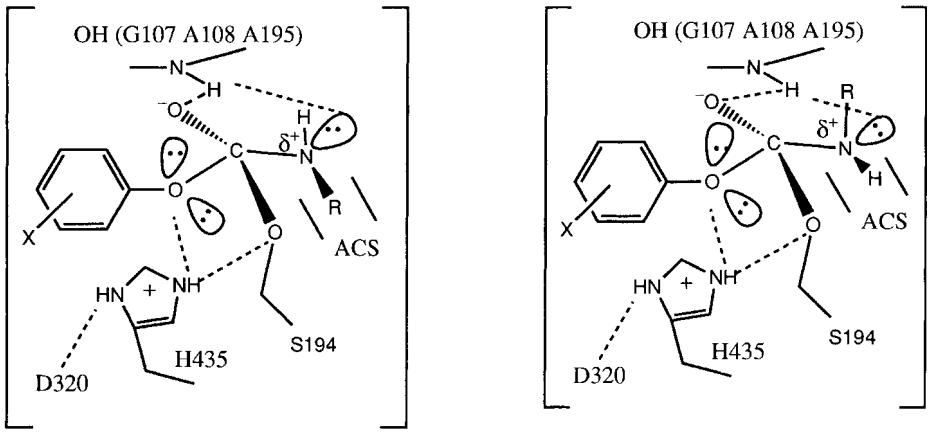

TD **11** TD **12**

Figure 5. Two possible tetrahedral adducts, TD **11** and TD **12**, for the inhibition of CEase by carbamates **1** and **2**. TD **11** and TD **12** are two most stable species owing to the lack of the rabbit-ears repulsion.[31] TD **11** is more stable than TD **12** because of the repulsion between the substituent R and S194 in TD **16** and the favorable interaction between the substituent R and ACS for in **11**

DISCUSSION

That the pK_a, log$k_{[OH]}$, δ_{NH}, $-\log K_i$ and logk_i values for carbamates **1** and **2** do not correlate with Eqn. (2) is probably due to the fact that the substituents at nitrogen (R) and at phenyl (X) (Fig. 1) do not contribute equally to the cross-interaction term. However, the pK_a, log$k_{[OH]}$, δ_{NH}, $-\log K_i$ and logk_i values show multiple linear correlations with σ_X, σ^* and $\alpha\sigma_X\sigma^*$ [Eqn. (3) and Table 2]. The α value in Eqn. (3) is defined to be 2.54 because the ρ^* for basic hydrolysis of benzolate ester, ArCOOEt, from the Hammett equation is 2.54.[25] Therefore, the contribution from the R substituent of carbamates **1** and **2** (Fig. 1) is 2.54-fold higher than that from the X substituent of carbamates **1** and **2** to the cross-interaction term because the substituent R is much closer to the reaction center than the substituent X (Fig. 1).

There are two possible conformations of carbamates **1** and **2** in solution, pseudo-*trans* and pseudo-*cis* conformers (Fig. 2). The $|\rho_{XR}|$ value of δ_{NH} correlation is 0.5 and less than those of log$k_{[OH]}$, $-\log K_i$ and logk_i correlations (Table 2). Therefore, the distances between the substituents R and X of carbamates **1** and **2** in $CDCl_3$ are far away and the pseudo-*trans* conformers are dominant in the pseudo-*trans*–pseudo-*cis* equilibria (Fig. 2).

The $|\rho_{XR}|$ value for the pK_a correlation of carbamates **1** and **2** is the smallest one (0.3) (Table 2). Therefore, the distances between the substituents R and X of carbamates **1** and **2** in the transition states of the protonations of carbamates **1** and **2** are relatively longer than those of other systems studied (Table 2). Hence the transition states of the protonations of carbamates **1** and **2** are predicted to be TS **3** (Fig. 2). There are two possible reasons for this: (a) the pseudo-*trans* conformers are dominant in the pseudo-*trans*–pseudo-*cis* equilibria, which lead to TS **3** (Fig. 2), and (b) the lone pairs at the nitrogen atoms of the pseudo-*cis* conformers are not perpendicular to the C=O π bonds owing to the repulsion between the substituent R and the substituted phenyl group, which make TS **3** less stable than TS **4** (Fig. 2).

The basic hydrolysis of carbamates **1** and **2** proceeds via the *E*1*cB* mechanism (Fig. 3).[28–30] The rate-determining step of *E*1*cB* can be either the deprotonation step (the first step, $\rho_{XR} = 0$) or the formation step of isocyanate (the second step, $\rho_{XR} \neq 0$).[23,25,26] The non-zero ρ_{XR} value (-2.4) for the log$k_{[OH]}$ correlation (Table 2) confirms that the second step of this *E*1*cB* mechanism (Fig. 3) is the rate-determining step.[23] The $|\rho_{XR}|$ value for the log$k_{[OH]}$ correlation is the largest (2.4) in Table 2. Therefore, the distance between the substituents R and X of carbamates **1** and **2** in the transition states of the *E*1*cB* mechanism (Fig. 3) should be the shortest (TS **10** in Fig. 4) according to Lee's prediction.[23] The transition state of the *E*1*cB* mechanism for the basic hydrolysis of carbamates **1** and **2** is predicted to be TS **10** instead of TS **9** probably because **8** is more stable than **7** owing to the favorable antiperiplanar interaction between lone pair **a** and the anti-bonding of C—O σ bond in **8** (Fig. 4).[31] On the other hand, the repulsion between lone pair **b** and two lone pairs of the phenol oxygen makes compound **7** unstable.

Like all aryl *N*-alkyl carbamates,[12–19] carbamates **1** and **2** are characterized as pseudo-substrate inhibitors of CEase because these inhibitors meet three criteria proposed by Abeles and Maycock.[32] The enzyme can be protected from inhibition by carbamates **1** and **2** in the presence of a competitive inhibitor, trifluoroacetic acid (TFA).[33] Therefore, carbamates **1** and **2** are also characterized as the pseudo-substrate inhibitors that bind

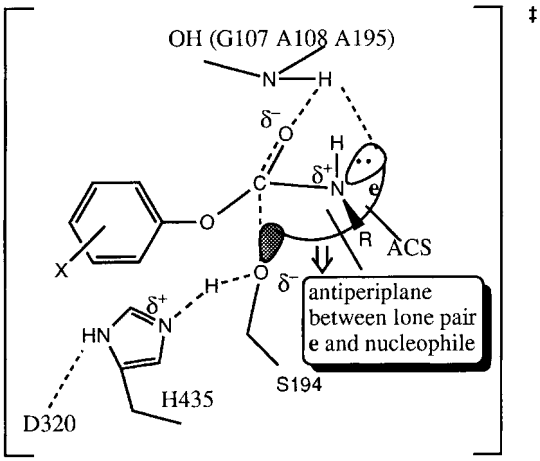

TS **13**

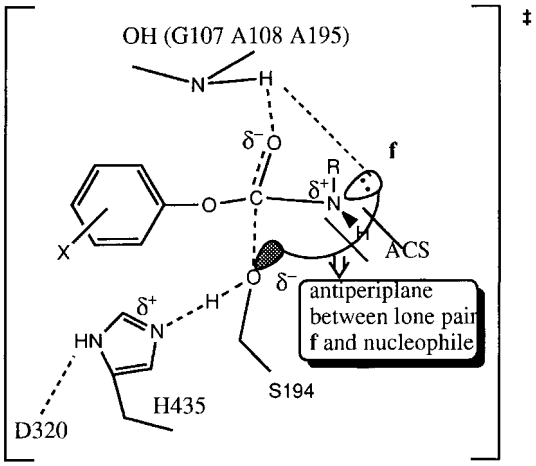

TS **14**

Figure 6. Two possible transition states, TS **13** and TS **14**, that lead to TD **11** and TD **12** (Fig. 5), respectively. TS **13** and TS **14** are two most stable species according to the prediction of the stereoelectronic effects.[31] TS **13** is more stable than TS **14** because of the repulsion between the substituent R and S194 in TS **14** and the favorable interaction between the substituent R and ACS in TS **13**

to the active site (ACS–ES–OH) of the enzyme (Fig. 1) (see *Return of activity and protection by TFA* in the Experimental section).[18,19] Since the ρ and ρ^* values for the CEase inhibitions by carbamates **1** and **2** have opposite signs,[14,16] the mechanisms for the CEase inhibitions by carbamates **1** and **2** may be different. In other words, the inhibition by carbamates **2** may not follow the same mechanism as shown in Fig. 1 owing to the negative ρ^* value for the $-\log K_i$ correlation, which apparently is not the character for the formation of the negative EI tetrahedral adduct (Fig. 1).[16] However, the common mechanism for the CEase inhibition by carbamates **1** and **2** (Fig. 1 and Scheme 1) is confirmed in this study because all $-\log K_i$, $\log k_c$ and $\log k_i$ values are correlated with Eqn. (3) (Table 2). Therefore, the CEase inhibition mechanisms by carbamates **1** and **2** are common (Fig. 1) and the K_i steps for the mechanisms should be further divided into two steps.

For the K_i step of the inhibition mechanism (Fig. 1), TD **11** and TD **12** (Fig. 5) are two very stable adducts because both lack any two-lone-pairs repulsion (the rabbit-ears interaction) based on stereoelectronic effects.[31] Stereoelectronic effects also predict that TS **13** and TS **14** (Fig. 6) are two very stable transition states because the lone pair on the nitrogen in both structures is at the antiperiplanar position for the direction of the nucleophile (serine) attack. TS **13** and TS **14** then react to form TD **11** and TD **12**, respectively. Based on the x-ray[10,11] and kinetic data[17–19] for CEase, TS **13** is a more favorable transition state than TS **14**, probably because the alkyl group of TS **13** is in ACS whereas the NH hydrogen of TS **14** is in ACS and the R substituent of TS **14** is in repulsion with the S194 nucleophile whereas this repulsion is lacking in TS **13** (Fig. 6). The large $|\rho_{XR}|$ value for the $-\log K_i$ correlation (2 ± 1) predicts that the distance between the substituents R and X in TS **13** is much closer than that in TS **14** and also confirms the fact that TS **13** is more stable than TS **14** (Fig. 6).

For the carbamylation (k_c) step, stereoelectronic effects predict that only two most stable TD **11** and TD **12** (Fig. 5) among six tetrahedral adducts are capable of forming the carbamyl enzymes because the antiperiplanar interaction between the lone pair of nitrogen and the anti-bonding orbital of the C—O σ bond is available in TS **15** and TS **16** (Fig. 7), which are from TD **11** and TD **12**, respectively.[31] Based on the x-ray[10,11] and kinetic data[17–19] for CEase, TS **15** is a more favorable transition state than TS **16**, probably owing to the favorable interaction between the substituent R of TS **15** and the ACS of the enzyme (Fig. 7). Therefore, the $|\rho_{XR}|$ value for the $\log k_c$ correlation (1 ± 1) predicts that the distance between the substituents R and X in TS **15** is much closer than that in TS **16**.

The k_c step is the rate-determining step for the overall inhibition mechanism (k_i) because all k_c values are much smaller than the $1/K_i$ values (Fig. 1 and Scheme 1).[12–17] Thus, TS **15** for the k_c step (Fig. 7) is less stable than TS **13** for the K_i step (Fig. 6). Since the ρ_{XR} value for the $\log k_i$ correlation is the sum of the values for both the $-\log K_i$ correlation and the $\log k_c$ correlation, the ρ_{XR} value for the $\log k_i$ correlation (2 ± 1) should be the greatest, that for the $\log k_c$ correlation (1 ± 1) should be the second and that for the $-\log K_i$ correlation (2 ± 1) should be the smallest. Although the experimental data are not completely confirmed (Table 2), the distance between the substituents R and X in TS **15** (Fig. 7) should be shorter than that in TS **13** (Fig. 6). Further evidence that supports the distance between the substituents R and X in TS **15** being shorter than that in TS **13** is that the latter has some coplanar, *trans* character for the substituents R and X from the starting pseudo-*trans*

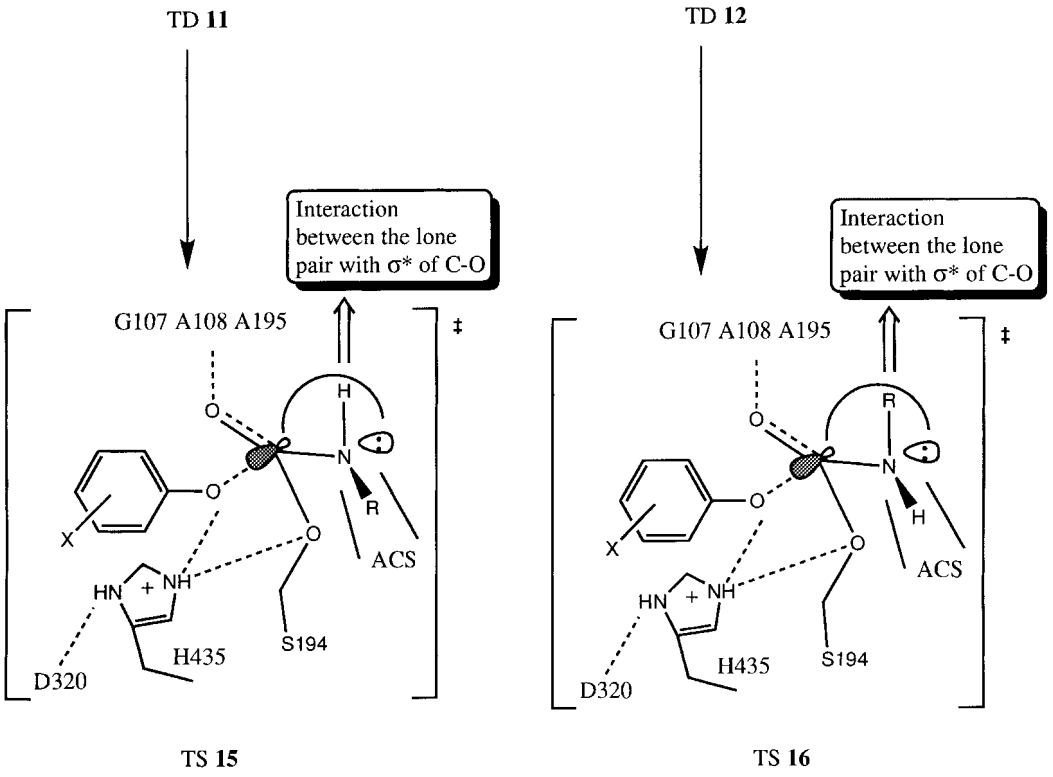

Figure 7. Two possible transition states, TS **15** and TS **16**, that lead to the carbamyl enzyme from the tetrahedral adducts, TD **11** and TD **12**, respectively. TS **15** is more stable than TS **16** based on similar reasons to those in Fig. 6

carbamates (Fig. 4), which make the distance of TS **19** longer than the distance of the more tetrahedral-like TS **15**.

Overall, the cross-interaction analyses of the structure–activity relationships allow us to propose the CEase inhibition mechanism by carbamates **1** and **2** shown in Fig. 8. First, the more stable pseudo-*trans* carbamates **1** and **2** diffuse into the enzyme to form the enzyme–inhibitor complex **16**. The lone pair of the carbamate nitrogen of complex **16** then rotates 90° around the C—N partial double bond to interact with the amide proton of OH (G107, A108 and G109) of the enzyme through the hydrogen bonding and to form the enzyme–inhibitor complex **17** that results in the development of the partial positive charge at the carbamate nitrogen of complex **17**. Therefore, the ρ^* value of the $-\log K_i - \sigma^*$ correlation for carbamates **2** is negative (-4 ± 2) (Table 2).[16] Complex **17** then leads to the tetrahedral adduct TD **11**, through the transition state TS **13** (Fig. 6). TD **11** then form the carbamyl enzyme pseudo-*cis*-**18**, through the transition state TS **15** (Fig. 7). Moreover, the large ρ_{XR} values for all inhibition data (Table 2) confirm the fact that the distances between the substituents R and X for all species in Fig. 8 except complex **16** are relatively shorter than the distance for pseudo-*trans* carbamates **1** and **2** (Fig. 1). Furthermore, the short distances between the substituents R and X for complex **17**, TS **13**, TD **11**, TS **15** and pseudo-*cis*-**18** strongly agree with the fact that the movements of all atoms in the CEase inhibition mechanism obey the principle of least nuclear motion (Fig. 8).[25,26]

From a rough MM-2 calculation using CSC Chem 3D, TS **4**, compound **8** and TS **10** are more stable than TS **3**, compound **7** and TS **9**, respectively (data not shown). Hence, the above prediction based on the rough MM-2 calculation also confirms the mechanisms in Figs 2 and 4 derived from the results of the Hammett–Taft cross-interactions. However, it is difficult to predict the relative stabilities among possible transition states or tetrahedral adducts for the CEase-catalyzed reaction by theoretical calculations owing to the huge molecular weight of the enzyme (63 ± 3 kDa).[11]

EXPERIMENTAL

Materials. All chemicals and biochemicals were of the highest grade available. CEase from porcine pancreas and *p*-nitrophenyl butyrate (PNPB) were obtained from Sigma; other chemicals were obtained from Aldrich. Silica gel used in liquid chromatography (Licorpre silica 60, 200–400 mesh) and thin-layer chromatographic plates (60 F_{254}) were obtained from Merck. The synthesis of carbamates **1** and **2** has been reported previously.[34]

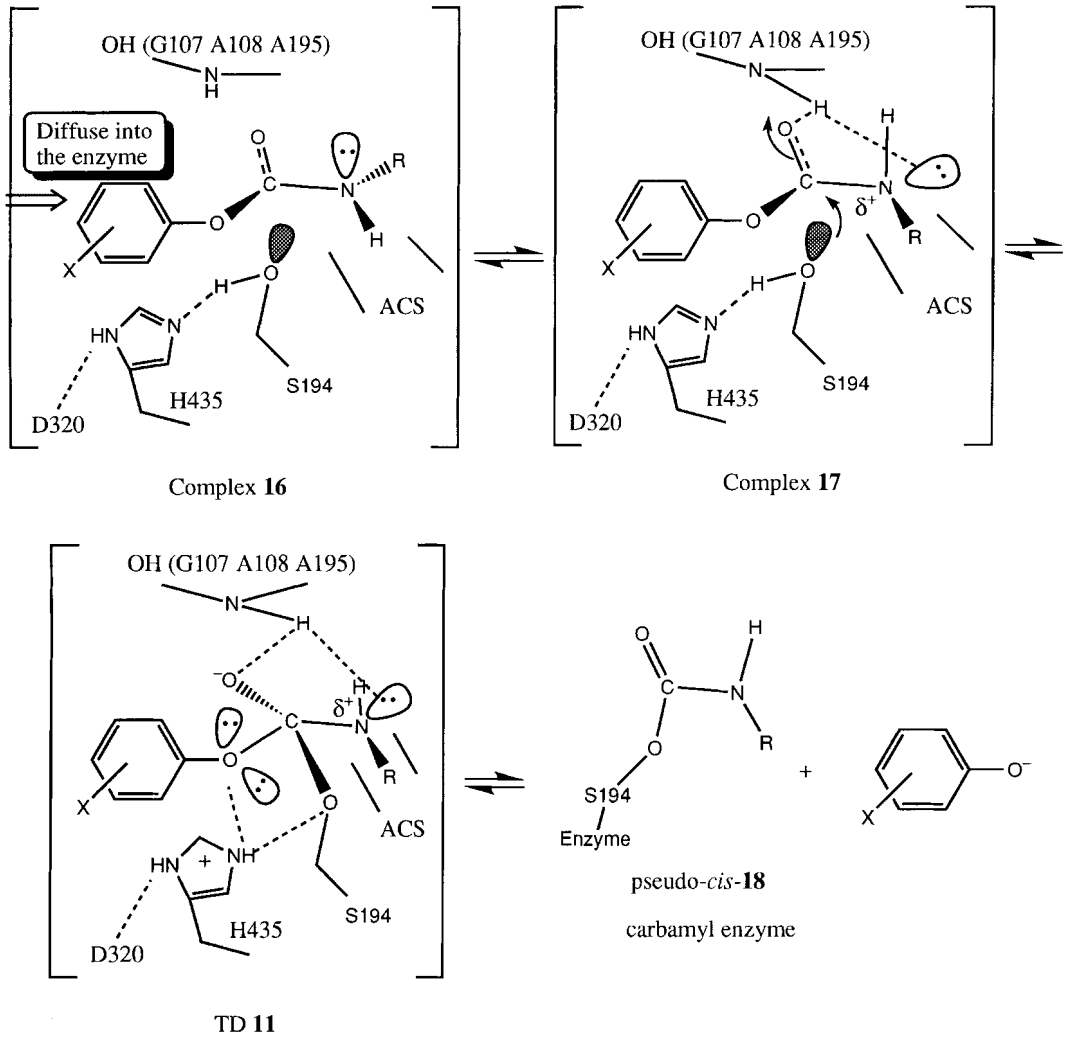

Figure 8. Proposed mechanism for the formation of the carbamyl enzyme, pseudo-*cis*-**18**, from carbamates **1** and **2** and CEase through complex **17** and TD **11**. The hydrogen bonding between the amide protons of OH and the lone pair of the carbamate nitrogen develops a partial positive charge at the carbamate nitrogen, which leads to a negative ρ^* value for the $-\log K_i$ correlation[16]

Instrumental methods. ^{1}H and ^{13}C NMR spectra were recorded at 300 and 75.4 MHz, respectively, on a Varian-XL 300 spectrometer. The ^{1}H and ^{13}C chemical shifts were referred to internal tetramethylsilane (TMS). Steady-state kinetic data were obtained with a UV–visible spectrophotometer (HP 8452 or Beckman DU-650) with a cell holder circulated with a water-bath. The pK_a values were obtained from pH-stat titration (Radiometer PHM 290).

Data reduction. Kaleida Graph (version 2.0) and Origin (version 4.0) were used for both linear and non-linear least-squares curve fittings. Stat Work and Origin were used for multiple linear least-squares regression analyses. CSC Chem 3D was used for the rough MM-2 calculation.

pK_a and $\log k_{[OH]}$. The pK_a values were obtained from the pH-stat titration. The values of $\log k_{[OH]}$ were obtained according to the procedures of Fujita *et al.*[28] The first-order rate constant, $k_{hyd.}$, of the acyl derivatives was obtained from the UV–visible spectrophotometric results, after calculation. The values of $\log k_{[OH]}$ were determined as the intercept of the plot of $\log k_{hyd}$ vs $\log[OH^-]$. The reaction temperature was kept at 25.0 ± 0.1 °C. All reactions were performed in sodium phosphate buffer (1 ml, 0.05 M, pH 8.0) containing NaCl (0.2 M), acetonitrile (2.5%, v/v), Triton X-100 (0.5%, w/w) and substrate (5 μmol). Reactions were monitored from 214 to 288 nm according to different absorptions of X—C_6H_4—OH.[29]

Steady-state enzyme kinetics. The steady-state CEase inhibitions were assayed by Hosie *et al.*'s method.[12–19] The temperature was maintained at 25.0 ± 0.1 °C by a refrigerated circulating water-bath. All reactions were performed in sodium phosphate buffer (1 ml, 0.1 M, pH

7.0) containing NaCl (0.1 M), acetonitrile (2%, v/v), Triton X-100 (0.5%, w/w), substrate (50 μM PNPB) and various concentrations (from 10^{-7} to 10^{-2} M for carbamates **1;** from 10^{-8} to 10^{-3} M for carbamates **2**) of inhibitors. Requisite volumes of stock solution of substrate and inhibitors in acetonitrile were injected into reaction buffers via a pipet. Porcine pancreatic CEase was dissolved in sodium phosphate buffer (0.1 M, pH 7.0). Reactions were initiated by injecting enzyme [50 μg or 1 unit (μmol min^{-1})] and monitored at 410 nm on the UV–visible spectrophotometer. First-order rate constants (k_{app} values) for inhibition of CEase were determined as described by Hosie *et al.* (Scheme 1).[12–19] Values of K_i and k_c can be obtained by fitting the data of k_{app} and [I] to Eqn. (4) by non-linear least-squares regression analyses:[12]

Duplicate sets of data were collected for each inhibitor concentration.

$$k_{app} = \frac{k_c[\mathrm{I}]}{K_i\left(1 + \frac{[\mathrm{S}]}{K_m}\right) + [\mathrm{I}]} \qquad (4)$$

Return of activity and protection by TFA. For the return of activity study, CEase (50 μg) was incubated with carbamate **1** or **2** (1 μM) in the absence and presence of TFA (2 μM),[33] a known competitive inhibitor of the enzyme before the inhibition reaction. The concentration of the substrate (PNPB) was 0.2 mM for CEase. All the other procedures followed those of Hosie *et al.*[12,13,17–19]

Acknowledgements

The author thanks the National Science Council of Taiwan for financial support and Cheng-Yue Lai, Wei-Cheng Liao and Bing-Hong Kuo for experimental data.

REFERENCES

1. Brockerhoff H, Jensen R-G. *Lipolytic Enzymes*. Academic Press: New York, 1974.
2. Fredrikzon B, Hernell O, Bläckberg L, Olivecrona T. *Pediatr. Res.* 1978; **12**:1048–1052.
3. Kritchevsky D, Kothari HV. *Adv. Lipid Res.* 1978; **16**:221–226.
4. Rudd EA, Brockman HL. In *Lipases*, Borgström B, Brockman HL (eds). Elsevier, Amsterdam, 1984.
5. Bhat SG, Brockman HL. *Biochem. Biophys. Res. Commun.* 1982; **109**:486–492.
6. Gallo LL, Clark SB, Myers S, Vohouny GV. *J. Lipid Res.* 1984; **25**:604–612.
7. Watt SM, Simmonds WJ. *J. Lipid Res.* 1981; **22**:157–165.
8. Brodt-Eppley J, White P, Jenkins S, Hui DY. *Biochim. Biophys. Acta* 1995; **1272**:69–72.
9. Svendsen A. In *Lipases, Their Structure Biochemistry and Application*, Woolley P, Petersen SB (eds). Cambridge University Press: Cambridge, 1994; 1–21.
10. Wang X, Wang C-S, Tang J, Dyda F, Zhang XC. *Structure* 1997; **5**:1209–1218.
11. Chen JC-H, Miercke LJW, Krucinski J, Starr JR, Saenz G, Wang X, Spilburg CA, Lange LG, Ellsworth JL, Stroud RM. *Biochemistry* 1998; **37**:5107–5117.
12. Hosie L, Sutton LD, Quinn DM. *J. Biol. Chem.* 1987; **262**:260–264.
13. Feaster SR, Lee K, Baker N, Hui DY, Quinn DM. *Biochemistry* 1996; **35**:16723–16734.
14. Lin G, Lai C-Y. *Tetrahedron Lett.* 1995; **36**:6117–6120.
15. Lin G, Liu H-C, Tsai Y-C. *Bioorg. Med. Chem. Lett.* 1996; **6**:43–46.
16. Lin G, Lai C-Y. *Tetrahedron Lett.* 1996; **37**:193–196.
17. Lin G, Tsai Y-C, Liu H-C, Liao W-C, Chang C-H. *Biochim. Biophys. Acta* 1998; **1388**:161–174.
18. Lin G, Shieh C-T, Tsai Y-C, Hwang C-I, Lu C-P, Chen G-H. *Biochim. Biophys. Acta* 1999; **1431**:500–511.
19. Lin G, Shieh C-T, Ho H-C, Chouhwang J-Y, Lin W-Y, Lu C-P. *Biochemistry* 1999; **38**:9971–9981.
20. Aldridge WN, Reiner E. In *Enzyme Inhibitors as Substrates*, Neuberger A, Tatun EL (eds). North-Holland: Amsterdam, 1972; 123–145.
21. Lee I, Sohn SC. *J. Chem. Soc, Chem. Commun.* 1986; 1055–1056.
22. Lee I, Kim HY, Kang HK. *J. Chem. Soc., Chem. Commun.* 1987; 1216–1217.
23. Lee I. *Adv. Phys. Org. Chem.* 1992; **27**:57–117.
24. Hine J. *Structural Effects on Equilibria in Organic Chemistry*. John Wiley & Sons: New York, 1975.
25. Isaacs NS. *Physical Organic Chemistry*. John Wiley & Sons: New York, 1987.
26. Lowry TH, Richardson KS. *Mechanism and Theory in Organic Chemistry* (3rd edn). Harper and Row: New York, 1987.
27. Connors KA. *Chemical Kinetics*. VCH: New York, 1990.
28. Fujita T, Kamoshita K, Nishioka T, Nakajima M. *Agric. Biol. Chem.* 1974; **38**:1521–1528.
29. Hall CD, Goulding CW. *J. Chem. Soc, Perkin Trans. 2* 1995; 1417–1477.
30. Broxton T, Chung RP-T. *J. Org. Chem.* 1995; **51**:3112–3115.
31. Deslongchamps P. *Stereoelectronic Effects in Organic Chemistry*. Pergamon Press: New York, 1983.
32. Abeles RH, Maycock AL. *Acc. Chem. Res.* 1976; 313–319.
33. Sohl J, Sutton LD, Burton DJ, Quinn DM. *Biochem. Biophys. Res. Commun.* 1988; **151**:554–560.
34. Lin G, Lai C-Y, Liao W-C. *Bioorg. Med. Chem.* 1999; **7**:2683–2689.